Polymer 54 (2013) 4093–4104

Contents lists available at SciVerse ScienceDirect

Polymer

journal homepage: www.elsevier.com/locate/polymer

Development of MWD and branching during peroxide modification of High-Density Polyethylene by SEC-MALS and Monte Carlo simulation

P.D. Iedema [a,*], K. Remerie [b], M. van der Ham [b], E. Biemond [b]

[a] Van 't Hoff Institute for Molecular Science, University of Amsterdam, Post Box 94157, 1090 GD Amsterdam, The Netherlands
[b] Sabic Europe, SABIC T&I, STC Geleen, Post Box 319, 6160 AH Geleen, The Netherlands

ARTICLE INFO

Article history:
Received 5 January 2013
Received in revised form
6 May 2013
Accepted 2 June 2013
Available online 13 June 2013

Keywords:
Polyethylene
Reactive processing
Chain length distribution

ABSTRACT

During the reactive processing of HD Polyethylene molecules are known to form branched structures, eventually resulting in a MFI decrease. This phenomenon was studied by experiments in a twin-screw extruder and measurement of the MWD by SEC-MALS. A Monte Carlo simulation model has been setup to calculate the MWD and branching distribution. The model includes both branching and random scission. Branch points are assumed to be created by coupling of vinyl ends of linear PE to secondary radical sites on PE backbones, yielding tertiary radical sites that undergo termination by disproportionation. This mechanism was recently proposed by Camara et al. [1]. Comparing the computed MWD to SEC-MALS data allowed determining the kinetic coefficients of the branching and scission reactions. Random scission turns out to be weak but still significant to prevent the formation of an extended MWD tail. For the found parameters perfect agreement was found between measured and computed MWD for various initial peroxide concentrations. These findings contribute to a better fundamental understanding of the simultaneous branching and scission during PE modification. It forms a firm support of the vinyl end to secondary radical coupling branching mechanism. Furthermore, it is shown that the MC simulations provide explicit branching topologies as a basis for predicting, for instance, complex rheological behavior of the modified polymer melt (Read et al. [2]).

1. Introduction

To improve product quality, industrially produced linear homo- and copolymers of Propylene and Ethylene are commonly subjected to chemical modification in extruders, chemically initiated by radical forming species like peroxides. It is commonly observed (Iedema et al. [3]) that Polypropylene simply degrades, as seen by an increase in the melt flow index (MFI). Obtaining branch points by chemical processing of PP requires special strategies (El Mabrouk et al. [4]). In radical modification PE branched structures are spontaneously created, eventually resulting in an MFI decrease. Terminal double bonds present in virgin PE take part in the system of radical reactions (Camara et al. [1]). Many other experimental results confirming branching are available in the open literature [5–15]. The effect of branching topology induced by reactive processing of polyolefin elastomer was undertaken recently by Liu et al. [16]. A number of modeling studies have been undertaken describing the development of the full distributions of molecular weight (MWD) and degree of branching (DBD) during the controlled degradation of PE [5,8–15]. Most of these papers make strongly simplifying assumptions, especially to deal with the problem of simultaneous scission and branching. Tobita [17–26] has presented a rigorous treatment of the latter problem indeed, using a special Monte Carlo simulations approach, but this approach does not fully address all the features of the PE modification problem.

The Monte Carlo simulation model reported here presents an approach that is equally rigorous as Tobita's, but in addition covers all the aspects of the full PE modification reaction system. For the first time, in this type of modeling, reactions are accounted for by radical groups that are created by scission or hydrogen abstraction and unsaturated groups, initially present in unmodified PE. This required developing a completely new Monte Carlo sampling scheme. The MC simulation model is validated to new data from PE modification experiments in a ZSK200 twin-screw extruder at Sabic Research. Thus, the model leads to a more quantitative understanding of the kinetic mechanisms involved, especially with respect to the way branches are created. This issue has been dealt with before in an electron paramagnetic resonance (EPR) spectroscopy study devoted to PE modification [1]. Our work confirms

* Corresponding author.
E-mail address: p.d.iedema@uva.nl (P.D. Iedema).

0032-3861/$ – see front matter © 2013 Elsevier Ltd. All rights reserved.
http://dx.doi.org/10.1016/j.polymer.2013.06.001

the findings from this study, be it in an entirely different manner. Moreover, the model allows computing the complete molecular weight and branching distribution. Thus, it directly gives access to finding the explicit branching topologies [27] that are so crucial for the hydrodynamic and rheological behavior [2,16]. In a recent Science paper [2] this MC simulation method has been shown, for the case of low-density Polyethylene, to successfully predict the complex melt rheology. The branching mechanism adopted in the present study is one of a few having been proposed in the literature [5–15]. These mechanisms have also been explored by us using an extended version of the MC model in a sensitivity study. The results of this study will be reported in a future paper.

In this paper the PE modification process is treated in a comprehensive manner as a system with simultaneous chain scission and branching. In general, such problems are not so easily solved using a deterministic population balance approach [27–29]. The main difficulty is attributed to the fact that the fragment size distribution resulting from the scission of branched polymer molecules depends on their size and number of branch points, but also on the branching topology in itself. In the context of PE modification this problem has been recognized and explicitly discussed by Gloor and Hamielec [7]. However, they did not solve the problem, but describe scission of the chains as if they were linear. Later, the group of Brandolin [5] addressed PE modification modeling using probability generating functions, again assuming linear scission. Most recently, the same group treated the problem while explicitly accounting for terminal unsaturation, but without the random chain scission reaction. By using a statistical approach, we avoid the explicit fragment size distribution problem encountered in the population balance.

This paper is structured as follows. First the experimental equipment with the ZSK200 twin-screw extruder and the characterization instruments like the SEC-MALS is presented. Then the model is introduced by presenting all the reactions involved. The population balance is inferred from this reaction system and it turns out to be a 6-dimensional one, if all the reactive groups are accounted for. The Monte Carlo simulation model to solve this problem is presented in the form of a flow diagram containing algorithms based on various probabilities. The values of the probabilities are shown to follow from balance equations of all the reactive groups involved based on reaction kinetics. The MWD's resulting from the simulations are compared to those from SEC-MALS. Finally, the interesting branching distribution is discussed.

2. Experimental

2.1. Extrusion experiments

A High-Density Polyethylene grade from Sabic, PE 539123, was subjected to varying peroxide concentrations between 0.1 and 0.4 weight per cent in a ZSK200 twin-screw extruder. The peroxide used was Perkadox (coated on Polypropylene grains), the average barrel temperature was maintained at 210 °C and the average reaction time 30 s.

2.2. SEC-MALS

We have employed SEC-MALS to determine the MWD of the linear unmodified PE and the branched PE samples. Using size exclusion chromatography, the macromolecules are separated according to hydrodynamic volume. In combination with light scattering, the absolute molar mass can be determined at each retention volume. Thus, the effect that branched polymer molecules have higher mass than linear ones is accounted for [30]. Employing SEC-MALS for determining the Molecular Weight Distribution of PE requires special high-temperature equipment and careful handling to avoid degradation. The procedure as described in Tackx & Tacx [30], for low-density Polyethylene, has now been applied to the present PE samples and it was carried out in the same laboratory (DSM Resolve, Geleen, NL). The polymer samples were dissolved (0.9 mg/ml) in 1,2,4-trichlorobenzene (TCB), which was distilled prior to use, over a period of 4 h at 150 °C and stabilized with butylated hydroxytoluene (BHT) at a concentration of 1 mg/ml. The solutions were filtered at high temperature (150 °C) using a millipore filtration setup (1.2 μm) positioned in a Hereous LUT oven operating at 150 °C.

The separation of the polymer according to molar mass is performed with a Polymer Laboratories PL GPC210. This SEC system is operated at high temperature (column compartment at 160 °C, injector compartment at 160 °C, and solvent reservoir at 35 °C), and a flow of 0.5 ml/min. Eluent is 1,2,4-trichlorobenzene. Two Polymer Laboratories SEC columns with large particle size (PLGel mixed A-LS 20 μm columns) in series are used to minimize shear degradation of high molar mass polymer chains [31]. The light scattering detector (a WYATT DAWN EOS multi-angle laser light scattering detector) is placed in line between the SEC and the refractive index detector. The used $dn/dc = 0.097$ ml/g. The measured MWD's are presented in Fig. 9.

2.3. Determination of end groups and unsaturations

Proton NMR and FTIR have been used to identify end groups and unsaturations. For NMR all the samples were dissolved at 120 °C in TCE containing di-tertbutylparacresol (DBPC) as stabilizer. The ^{1}H NMR spectra were recorded at 120 °C on a 500 MHz instrument. Both branching and unsaturations (trans, chain end and side groups) have been determined by FTIR, using a Perkin Elmer Spectrum One. The presence of vinyl end groups has been identified, decreasing from ^{13}C=C per 10^5 C-atoms for untreated PE, to 6 for the highest peroxide concentrations.

3. Modeling

3.1. Dimensionality and reaction mechanisms

The reaction mechanisms involved in the controlled degradation of PE will be listed in this section. The major part of these reactions with PE has been reported elsewhere [5–15]. The reaction equations are expressed in terms of a 6-dimensional distribution variable representing all the polymer molecules acting in this radical system: $P_{n,b,v,p,s,t}$. This dimensionality is not an a priori given, but it follows from the mechanisms that we want to account for in our model, as shown below. The indices refer to, resp.: n, number of monomer units, b, number of branch points, v, number of terminal unsaturations (vinyl end), p, number of primary radical sites, s, number of secondary radical sites, t, number of tertiary radical sites. These 6 properties together form the minimum set, since on the one hand they represent the macromolecular descriptors that we are interested in (numbers of units and branch points), and on the other they determine the molecule's reactivity (vinyl groups). Note that we account for 'multiradical' molecules, although in this case of relatively mild PE degradation quantities of molecules with more than one radical may be still relatively low. Multiradicals are becoming important, if the focus is shifted to gelation, as has been reported in previous work [32].

3.2. Reactions taken into account in the model

The following list of reaction mechanisms involved in PE modification represents the initiation, propagation and termination reactions that are commonly supposed to be acting in radical induced

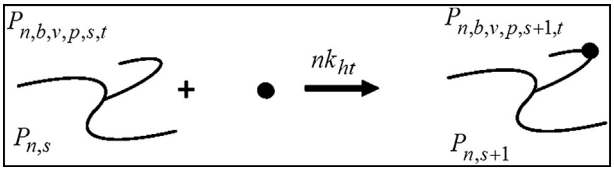

Fig. 1. Hydrogen abstraction.

degradation of polyolefins. Reactions involving macromolecules are depicted in Figs. 1–5.

Peroxide dissociation

$$I_2 \xrightarrow{k_d} 2I^{\bullet} \tag{1}$$

Hydrogen abstraction by initiator radicals (Fig. 1)

$$P_{n,b,v,p,s,t} + I^{\bullet} \xrightarrow{nk_{ht}} P_{n,b,v,p,s+1,t} \tag{2}$$

Henceforth, we will employ a shorthand notation, in which only the properties involved in the reaction will be written. Thus, reaction Eq. (2) becomes:

$$P_{n,s} + I^{\bullet} \xrightarrow{nk_{ht}} P_{n,s+1}$$

Hydrogen abstraction by molecules with primary radical sites (Fig. 2):

$$P_{n_1,s_1} + P_{v_2,p_2} \xrightarrow{n_1 k_{htp}} P_{n_1,s_1+1} + P_{v_2+1,p_2-1} \tag{3}$$

Disproportionation of molecules with primary radical sites and other macroradicals, leading to vinyl groups (Fig. 3):

$$P_{v_1,p_1} + P_{v_2,p_2} \xrightarrow{p_1 p_2 k_{td}} P_{v_1+1,p_1-1} + P_{v_2,p_2-1} \tag{4a}$$

$$P_{v_1,p_1} + P_{v_2,s_2} \xrightarrow{p_1 s_2 k_{td}} P_{v_1+1,p_1-1} + P_{v_2,s_2-1} \tag{4b}$$

$$P_{v_1,p_1} + P_{v_2,t_2} \xrightarrow{p_1 t_2 k_{td}} P_{v_1+1,p_1-1} + P_{t_2,p_2-1} \tag{4c}$$

Scission and branching are assumed to be taking place according to the mechanisms described below. It may be realized that regarding branching a number of mechanisms has been proposed in the literature on PE modification [5–15]. The choice we have made here, vinyl to secondary radical coupling, is based on a sensitivity study using an extended version of the MC model. The results of this study will be reported in a future paper.

Chain scission at secondary radical sites (Fig. 4):

$$P_{n,b,v,p,s} \xrightarrow{sf(n,n_1,b,b_1,\text{topology})k_s} P_{n_1,b_1,v_1,p_1,s_1} + P_{n-n_1,b-b_1,v-v_1+1,p-p_1+1,s-s_1-1} \tag{5}$$

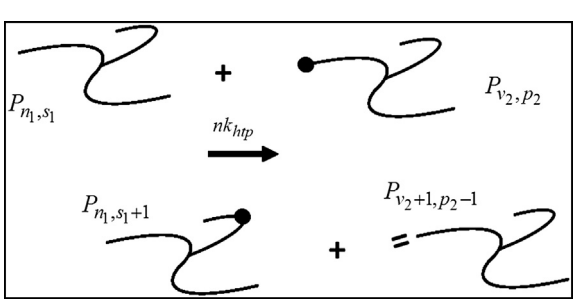

Fig. 2. Hydrogen abstraction by primary macroradicals yielding secondary macroradicals.

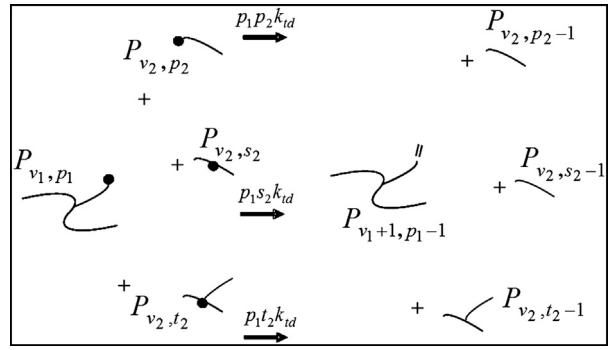

Fig. 3. Disproportionation of primary macroradicals and other macroradicals, leading to vinyl groups.

Vinyl group coupling to secondary radical site yielding tertiary radical sites (Branch formation, Fig. 5)

$$P_{b_1,v_1,s_1,t_1} + P_{b_2,v_2,s_2,t_2} \xrightarrow{v_1 s_2 k_{vs}} P_{b_1+b_2+1,v_1+v_2-1,s_1+s_2-1,t_1+t_2+1} \tag{6}$$

3.3. Discussion of the reaction mechanisms

As regards the *hydrogen abstraction* reactions, Eqs. (2) and (3), note that the reaction rate is proportional to the number of monomer units in the dead polymer molecule, n; index s is increased by one, referring to the increase of the number of secondary radical sites. The 3 disproportionation reactions take place between all of the 3 radical site types, Eq. (4). Reactions between *primary* radical sites and all radical sites are yielding *vinyl groups*. Consequently, in the reaction equations the index referring to unsaturations on one of the molecules increase by one, while the number of radical sites on both decrease by one.

Scission is assumed to take place at a secondary radical site (Eq. (5)). Note that scission is responsible for molecular size *reduction*, but by creating fragments with reactive groups that may take part in a subsequent branching reaction, they indirectly contribute to size *growth*. The rate coefficient, apart from the Arrhenius coefficient, k_s, contains a complex function due to the branched structure, which will be explained below. The scission reaction according to Eq. (5) yields fragments with primary radical sites and vinyl groups, which is reflected in the *sum* of index values of the fragments, $p_1 + (p - p_1 - 1) = p + 1$, resp. $v + 1$, while the sum of indices referring to the secondary radical sites is diminished by one: $s - 1$. The rate function in Eq. (5) clearly illustrates the complexity of the random scission of branched structures. The deterministic solution of this problem [27–29] has been extensively addressed and an important difficulty was found to deal with the scission rate, which is different for polymers of different dimensions. This rate turns out to be a function of: a) the numbers of monomer units and branch points on both the original polymer molecule (n,i) and the fragments (m,j); and b) the *branching topology* of the original polymer

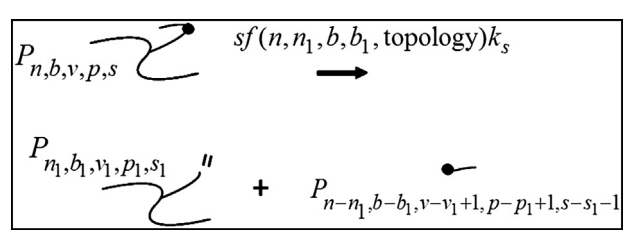

Fig. 4. Random scission of secondary macroradical leading to a primary radical and a vinyl end.

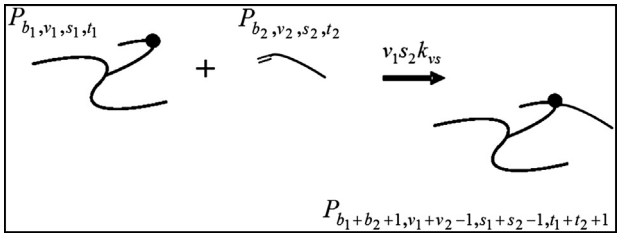

Fig. 5. Vinyl group coupling to secondary radical site yielding tertiary macroradical branch points.

structure. This scission function, *f*(*n*,*m*,*i*,*j*,topology), is not a priori known. It may be approximated by an empirical equation, as has been done for other (simpler) systems. However, as we will discuss below, the present case allows separating the scission and branching problem without loss of generality.

Branch points are created as tertiary radical sites by reactions according to Eq. (6) by the coupling between *vinyl groups and secondary radical sites*. This reaction has been proposed recently [1]. It contributes to branching and growth of molecules without prerequisite scission.

3.4. Monte Carlo simulation model

3.4.1. Solution strategy

The 6-dimensional population balance resulting from the reaction mechanisms taken into account does not have to be solved in this high-dimensional form. In the first place we will separate the scission from the branching problem. This is allowed since all bonds between monomer units constituting the polymer present in the reactor are supposed to be equally intensively exposed to the scission reaction. The problem is then reduced to characterizing the linear scission fragments according to scission kinetics and subsequently constructing the branched polymers according to the branching kinetics. The latter process is depicted in Fig. 6. It should be noted that this represents a *simulated* growth process that nevertheless includes all the essential elements of the real growth process. The lengths of the linear segments and the nature of their end points are those of the linear PE molecules *after* scission. Therefore, some of the vinyl ends may originate from the virgin PE material, while others may have resulted from scission and subsequent termination. Note furthermore, that the secondary radical sites are not explicitly featuring in this model representation. For the model it is sufficient to ensure that any monomer unit of a polymer molecule has equal probability of becoming a secondary radical site and undergo a subsequent branching reaction. Consequently, the reactivity of a molecule is proportional to its number of monomer units.

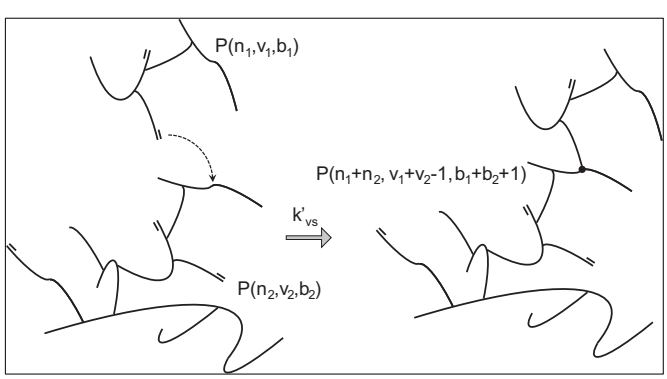

Fig. 6. Simulated growth step of branched molecule by coupling of vinyl end to secondary radical site on chain backbone. Number of secondary radical sites proportional to number of monomer units in molecule, *n*. Length of linear segments and end type (vinyl or saturated) representative of the state *after* scission. Here, $v_1 = 2$, $b_1 = 3$; $v_2 = 3$, $b_1 = 8$; after reaction step $v = 4$, $b = 12$. Created branch point is highlighted.

3.4.2. Determining length distribution of PE segments after scission

The characteristics of the linear PE segments are obtained in an efficient manner using a *semi-analytical* approach developed by us before [27,28]. The required equations have been listed in Table 1. They employ the average probability of a bond between monomer units to undergo scission, also called the scission density, ρ_s. Since scission takes place at secondary radical sites, the instantaneous rate of the scission reaction equals $k_s\lambda_1^s(t)$. Here, $\lambda_1^s(t)$ represents the total concentration of secondary radical sites that follows as a first moment from the original 5-dimensional concentration distribution as:

$$\lambda_1^s = \sum_{s=0}^{\infty} s \sum_{n,b,v,p,t}^{\infty} \cdots\cdots \sum^{\infty} P_{n,b,v,p,s,t} \tag{7}$$

The total molar number of scissions is calculated by integrating $\lambda_1^s(t)$ over reaction time and then the scission density follows after division by the total number of monomer units, μ_1:

$$\rho_s = \frac{k_s}{\mu_1} \int_0^{\tau} \lambda_1^s \mathrm{d}t \tag{8}$$

Here μ_1 is defined as:

$$\mu_1 = \sum_{n=1}^{\infty} n \sum_{b,v,p,s,t}^{\infty} \cdots\cdots \sum^{\infty} P_{n,b,v,p,s,t} \tag{9}$$

Note that the total number of monomer units remains constant during the modification process.

In view of the reactions involved, hydrogen transfer (by initiator and primary radicals), termination and vinyl to secondary radicals site coupling, $\lambda_1^s(t)$ obeys the following balance:

$$\frac{\mathrm{d}\lambda_1^s}{\mathrm{d}t} = k_{ht}\mu_1 \mathrm{I}^\bullet + k_{htp}\mu_1\lambda_1^p - \lambda_1^s\left\{k_s + k_{td}\lambda_1^p + k_{tds}\left(\lambda_1^p + \lambda_1^s + \lambda_1^t\right) + k_{tdt}\lambda_1^t + k_{vs}\mu_1^v\right)\right\} \tag{10}$$

Here $\mathrm{I}^\bullet$ denotes the peroxide radical concentration, described by the balance equation:

$$\frac{\mathrm{d}\mathrm{I}^\bullet}{\mathrm{d}t} = 2k_d \mathrm{I}_2(0)\exp(k_d t) - k_{ht} m \mathrm{I}^\bullet - k_i \mu^v \mathrm{I}^\bullet \tag{11}$$

$\mathrm{I}_2(0)$ denotes the initial peroxide concentration, while the exponential function refers to the 1st-order decay of the I_2-concentration according to the dissociation reaction, Eq. (1). The two last terms express the peroxide radical consumption by the hydrogen abstraction and the terminal unsaturation activation reaction, resp. The further moments in the equations above are derived from the 5-dimensional distribution as:

Total number of terminal unsaturation (vinyl groups):

$$\mu_1^v = \sum_{v=0}^{\infty} v \sum_{n,b,p,s,t}^{\infty} \cdots\cdots \sum^{\infty} P_{n,b,v,p,s,t} \tag{12}$$

Total number of primary radical sites:

Table 1
Equations from the semi-analytical approach describing fractions of chains with varying numbers of scission points and length distributions of chains [27,28].

Weight fractions of chain fragments with 0, 1 and 2 scission end points
$p_i^{wt} = \sum_{n=1}^{\infty} f_i(n) P_n n/\mu_1$
$f_0(n) = \exp(-n\rho_s)$
$f_1(n) = 2/n\rho_s - 2(1+1/n\rho_s)\exp(-n\rho_s)$
$f_2(n) = (1-2/n\rho_s) + (1+2/n\rho_s)\exp(-n\rho_s)$
Length distributions of chain fragments with 0, 1 and 2 scission end points
$p^{wt}(n\|0) = P_n n \ \exp(-n\rho_s)/\sum_{n=1}^{\infty} P_n n \ \exp(-n\rho_s)$
$p'(n\|1) = 2\rho_s \ \exp(-n\rho_s)\sum_{n'=n}^{\infty} P_{n'}; \quad p^{wt}(n\|1) = p'(n\|2)/\sum_{n=1}^{\infty} p'(n\|1)$
$p'(n\|2) = \rho_s^2 n \ \exp(-n\rho_s)\sum_{n'=n}^{\infty}(n'-n)P_{n'}; \quad p^{wt}(n\|2) = p'(n\|2)/\sum_{n=1}^{\infty} p'(n\|2)$
Conditional number fractions of chains ending with 0 and 1 scission points
$f(1\|0,n) = 1-\exp(-n\rho_s); \quad f(0\|0,n) = 1-f(1\|0,n)$
$f(1\|1,n) = 1-1-\exp(-n\rho_s)/n\rho_s; \quad f(0\|1,n) = 1-f(1\|1,n)$
$p^{nr}(i\|j) = \sum_{n=1}^{\infty} f(i\|j,n) P_n n/\mu_1$
Conditional length distributions of chains ending with 0 and 1 scission points
$p^{nr}(n\|0,0) = P_n \ \exp(-n\rho_s)/\sum_{n=1}^{\infty} P_n \ \exp(-n\rho_s)$
$p^{nr}(n\|1,0) = \exp(-n\rho_s)$
$p^{nr}(n\|0,1) = p^{nr}(n\|1,0)$
$p'(n\|1,1) = \rho_s \ \exp(-n\rho_s)\sum_{n'=n}^{\infty}(n'-n)P_{n'}; \quad p^{nr}(n\|1,1) = p'(n\|1,1)/\sum_{n=1}^{\infty} p'(n\|1,1)$
$\mu_0 = \sum_{n=1}^{\infty} P_n; \quad \mu_1 = \sum_{n=1}^{\infty} P_n n$

$$\lambda_1^p = \sum_{p=0}^{\infty} p \sum_{n,b,v,s,t}^{\infty} \cdots\cdots \sum^{\infty} P_{n,b,v,p,s,t} \tag{13}$$

Total number of tertiary radical sites:

$$\lambda_1^t = \sum_{t=0}^{\infty} s \sum_{n,b,v,p,s}^{\infty} \cdots\cdots \sum^{\infty} P_{n,b,v,p,s,t} \tag{14}$$

These moments follow from the following set of balance equations.

Primary radical sites:

$$\frac{d\lambda_1^p}{dt} = k_s\lambda_1^s + k_i\mu_1^v I^\bullet - \lambda_1^p\left\{k_{htp}\mu_1 + k_{td}\left(\lambda_1^p + \lambda_1^s + \lambda_1^t\right) + k_{tds}\lambda_1^s + k_{tdt}\lambda_1^t\right\} \tag{15}$$

Secondary radical sites:

$$\frac{d\lambda_1^s}{dt} = k_{ht}mI^\bullet + k_{htp}m\lambda_1^p - \lambda_1^s\left\{k_s + k_{td}\lambda_1^p + k_{tds}\left(\lambda_1^p + \lambda_1^s + \lambda_1^t\right) + k_{tdt}\lambda_1^t + k_{vs}\mu_1^v\right\} \tag{16}$$

Tertiary radicals:

$$\frac{d\lambda_1^t}{dt} = k_{vs}\lambda_1^s\mu_1^v - \lambda_1^t\left\{k_{td}\lambda_1^p + k_{tds}\lambda_1^s + k_{tdt}\left(\lambda_1^p + \lambda_1^s + \lambda_1^t\right)\right\} \tag{17}$$

Terminal vinyl groups

$$\frac{d\mu_1^v}{dt} = k_s\lambda_1^s + k_{td}\lambda_1^p\left(\frac{1}{2}\lambda_1^p + \lambda_1^s + \lambda_1^t\right) + k_{htp}m\lambda_1^p - \mu_1^v k_{vs}\lambda_1^s \tag{18}$$

Note that since branch points are created by termination of tertiary radicals the consumption term in Eq. (17) represents the rate of creation of branch points, b. This quantity is related to the 6D concentration distribution after:

$$\mu_1^b = \sum_{b=0}^{\infty} b \sum_{n,v,p,s,t}^{\infty} \cdots\cdots \sum^{\infty} P_{n,b,v,p,s,t} \tag{19}$$

Furthermore, as generally in radical systems the concentration of macroradicals is sufficiently low to permit a *quasi-steady state approximation*, which renders the accumulation term, dx/dt, equal to zero. Thus, from Eq. (17), we see that the branch point creation rate is well approximated by:

$$\frac{d\mu_1^b}{dt} = k_{vs}\lambda_1^s\mu_1^v \tag{20}$$

3.4.3. Model to create branched molecules from linear segments after scission

The linear PE segments with characteristics according to Table 1 now have to be combined in order to construct the branched molecules. This branching problem in the model representation of Fig. 6 may be formulated as the following population balance in 3 dimensions: chain length, n, number of vinyl ends, v, and number of branch points, b:

$$\frac{dP(n,v,b)}{dt} = k'_{vs}\sum_{n'}^{n-1}\sum_{v'}^{v}\sum_{b'}^{b} n'(v-v'+1)P(n',v',b') \times P(n-n',v-v'+1,b-b'-1) - k'_{vs}\mu_1^v\mu_1 nvP(n,v,b) \tag{21}$$

Here, the rate coefficient represents the effective rate coefficient by which smaller molecules 're combined to larger ones by connecting them through branch points. Taking the summation of Eq. (21), $\sum_{n=1}^{\infty}\sum_{v=0}^{\infty}\sum_{b=0}^{\infty} b\,dP(n,v,b)/dt$ should reproduce the same rate of creation of branch points as Eq. (20). Therefore, the effective branching coefficient, k_{vs}', is related to the kinetic coefficient by:

$$k'_{vs} = \frac{\lambda_1^s}{\mu_1}k_{vs} \tag{22}$$

Solving the 3D-population balance Eq. (21) in a deterministic manner would require sophisticated means to compute the convolution term as shown by us elsewhere [29]. At this point we decided to obtain the solution by a Monte Carlo sampling method. This method has been applied on a similar, but simpler problem before [19]. We have now developed a new method based on the same principles.

The linear PE segments after scission are called *primary polymers* [17]. A flow chart of the algorithm is shown in Fig. 7. The procedure starts with one primary polymer in generation 0. It may be connected in two ways: somewhere along its *backbone* to the end points of other primary polymers and at its *end points* to an

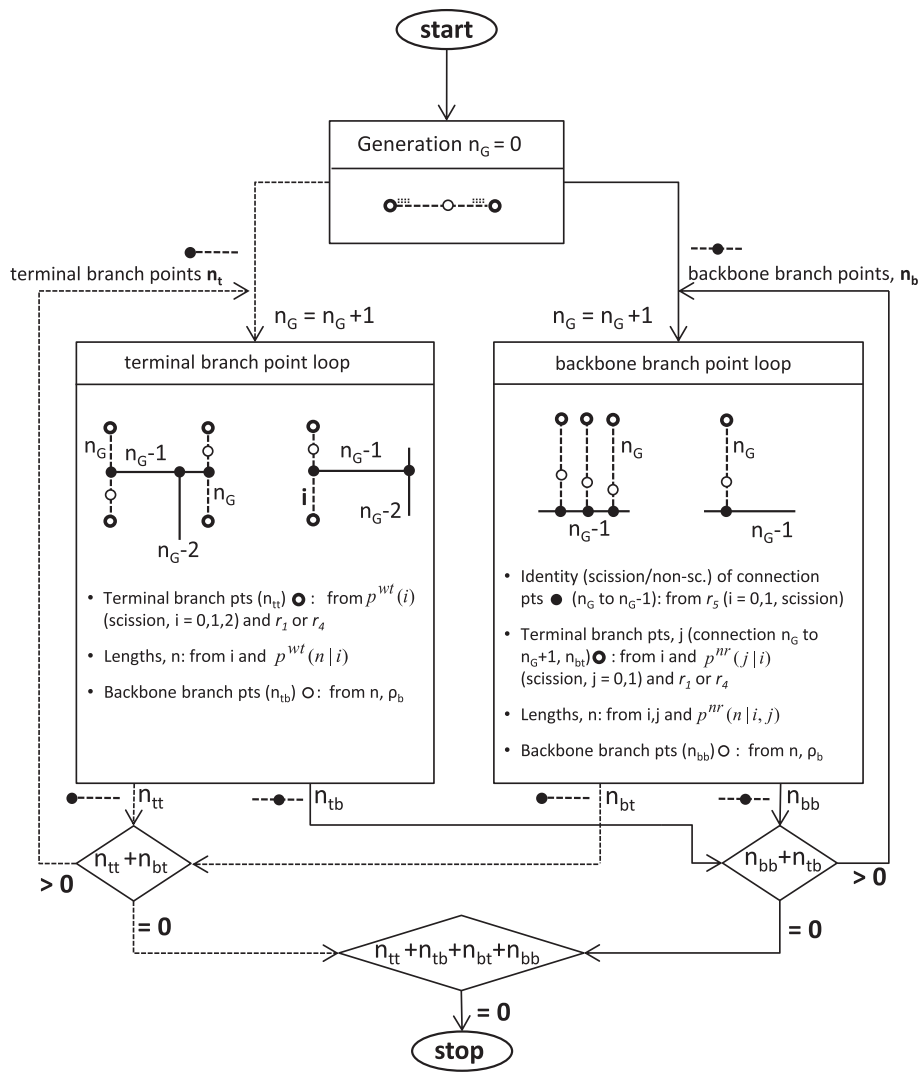

Fig. 7. Flow chart of the Monte Carlo simulation model. The algorithm starts in generation $n_G = 0$ with one primary polymer. This and all subsequent primary polymers may have branch points on their backbone (open thin circles) or at its two end points (open fat circles). This is determined in the *terminal branch point loop*. Once the branch points are identified (denoted by black circles), they enter into the 2 different blocks for the next generation as *terminal* or as *backbone* branch points. Within the blocks the lengths as well as the branch points for the next generations are determined, using the probability distributions from the kinetic model and Table 1.

arbitrary unit on the backbone of other primary polymers. Determining the two types of connectivity takes place in the two blocks of Fig. 7. Some tasks performed in these loops are common, some others are specific. We will first address the two common tasks: determining whether an *end point* of a primary polymer is a branch point and computing the number *backbone branch points* on a primary polymer.

3.4.4. End point connectivity

The primary polymer in generation 0 and all other primary polymers, connected by backbone or end point, may have branch points on their *end point*. As goes from Fig. 7, for each backbone connected primary polymer *two* end points are to be evaluated, for each end point connected chains just *one*. The connectivity of an end point is determined as follows. An end point may only become connected as a vinyl end reacting with a secondary radical. Such a vinyl end may have been present from the start as an *initial* one, not having undergone scission, or be *created by scission*.

In the case of a non-scission end we need the initial fraction of all end points being a vinyl end, $r_=(0)$, as well as the probability that this type of vinyl end has reacted to a connection point. The concentration of such vinyl ends, μ_1^{v0}, being consumed by the branching reaction, is described by the balance:

$$\frac{d\mu_1^{v0}}{dt} = -k_{vs}\mu_1^{v0}\lambda_1^s \quad t = 0: \quad \mu_1^{v0}(0) = 2r_=(0)\mu_0(0) \tag{23}$$

Here, $\mu_0(0)$ is the concentration of polymer chains at $t = 0$ as defined by:

$$\mu_0(0) = \sum_{n,b,v,p,s,t}^{\infty} \cdots\cdots \sum^{\infty} P_{n,b,v,p,s,t}(0) \tag{24}$$

The amount of terminal vinyl groups from virgin PE reacting to branch points thus equals $k_{vs}\int_0^\tau \mu_1^{v0}\lambda_1^s dt$. Hence, the probability that a chain end, not having undergone scission, is an originally present vinyl end converted into a branch point, r_1, follows as:

$$r_1 = \frac{k_{vs}\int_0^\tau \mu_1^{v0}\lambda_1^s dt}{\mu_1^{v0}(0)} r_=(0) \tag{25}$$

If the chain end happens to be created by scission, then there is a probability that it changes into a vinyl end that reacts with a secondary radical site and becomes a branch point. This sequence of reactions is shown in Fig. 8. Upon scission an amount of vinyl ends is *directly* created, equal to $k_s \int_0^\tau \lambda_1^s \mathrm{d}t$, apart from the same amounts of primary radicals. As described by Eq. (2) primary radical sites terminate by disproportionation and hydrogen abstraction reactions, a part of this *indirectly* yielding vinyl ends. This fraction is given by:

$$r_2 = \frac{\int_0^\tau \lambda_1^p \left\{ k_{td}\left(\frac{1}{2}\lambda_1^p + \lambda_1^s + \lambda_1^t\right) + k_{htp}\mu_1 \right\} \mathrm{d}t}{\int_0^\tau \lambda_1^p \left\{ k_{htp}\mu_1 + k_{td}\left(\lambda_1^p + \lambda_1^s + \lambda_1^t\right) + k_{tds}\lambda_1^s + k_{tdt}\lambda_1^t \right\} \mathrm{d}t} \tag{26}$$

Furthermore, the fraction of terminal vinyl groups originating from scission reacting to branch points is given by:

$$r_3 = \frac{k_{vs} \int_0^\tau \mu_1^v \lambda_1^s \mathrm{d}t}{\int_0^\tau \left\{ k_s \lambda_1^s + k_{td}\lambda_1^p \left(\frac{1}{2}\lambda_1^p + \lambda_1^s + \lambda_1^t\right) + k_{htp}\mu_1\lambda_1^p \right\} \mathrm{d}t} \tag{27}$$

Here, it should be noted that the concentration of the vinyl ends created by scission and consumed by the branching reaction, μ_1^v, is given by Eq. (18), if this differential equation is solved for an initial condition $\mu_1^v(0) = 0$. Thus, the overall probability of a scission end to become a branch point follows as:

$$r_4 = (0.5r_2 + 1)r_3 \tag{28}$$

The determination of terminal branch points is required in both the terminal branch and the backbone branch loop. The number of such branch points connects the primary polymers of generation n_G to an equal number of primary polymers in generation $n_G + 1$. The latter primary polymers are evaluated by entering the subsequent part of the algorithm in the *terminal branch point loop* (see Fig. 7).

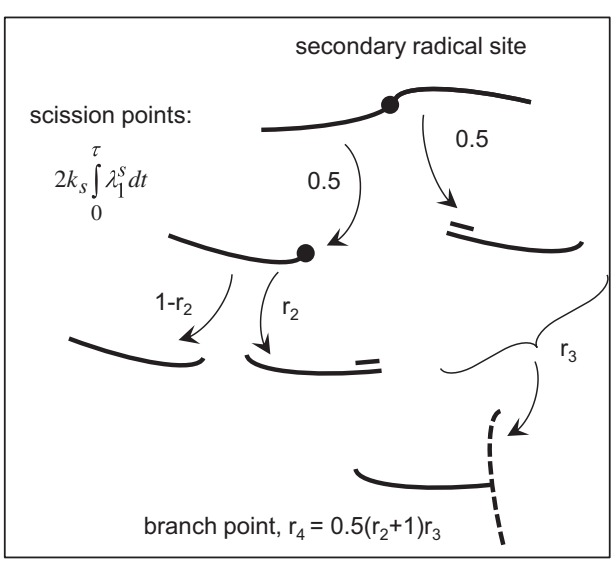

Fig. 8. Sequence of reactions following the scission of a chain at a secondary radical site. Vinyl ends are formed both directly upon scission as via primary radicals. Ultimately they may form a branch point, with a probability r_4 (Eq. (28)).

3.4.5. Backbone connectivity

The primary polymer in generation 0 and all other primary polymers, either connected by backbone or end point, may have branch points on their *backbone*. This depends on the probability of a monomer unit of being a branch point, also called the average *branching density*, ρ_b, according to Eq. (20) defined as:

$$\rho_b = \frac{\mu_1^b}{\mu_1} = \frac{k_{vs}}{\mu_1} \int_0^\tau \lambda_1^s \mu_1^v \mathrm{d}t \tag{29}$$

The actual number of branch points, b, depends on ρ_b and on the sampled chain length, n, and follows by sampling from a binomial distribution:

$$p(b|n, \rho_b) = \binom{n}{b} (\rho_b)^b (1 - \rho_b)^{n-b} \tag{30}$$

The determination of backbone branch points is again required in both the terminal branch and the backbone branch loop. The number of such branch points connects the primary polymers of generation n_G to an equal number of primary polymers in generation $n_G + 1$. The latter primary polymers are evaluated by entering the subsequent part of the algorithm in the *backbone branch point loop* (see Fig. 7).

3.4.6. Terminal branch point loop

The procedure, also for the first segment, to determine its eventual connectivity at end points or backbone as well as its length, is depicted in the *terminal branch point loop* block in Fig. 7. This procedure is applied to the first primary polymer and to those sampled as being attached at an arbitrary unit at their backbone (black dots). Note that the primary polymer of generation 0 obviously has no such point as it does not possess a primary polymer of a *previous* generation to which it is attached.

Now first, the nature of the end points of the primary polymer, scission or non-scission, has to be determined. For both the generation 0 primary polymer as for a backbone connected primary polymer this happens by a sampling procedure that starts by picking an arbitrary unit along the backbone of the primary polymer. In the case of a backbone connected chain this obviously is the connection point. Then a procedure is applied to check whether scission has taken place at either side, given the scission probability ρ_s from Eq. (8). The result of this procedure is obtained using the *semi-analytical method* [27,28] and is shown in Table 1 as the *chain length weighted* probability distribution of finding i scission ends ($i = 0, 1$ or 2), $p^{wt}(i)$. If finally the nature of the end points is known, scission or non-scission, the probability that they are branch points follows using the probabilities r_1 and r_4 obtained above, by Eqs. (25) and (28), resp. The task is performed by picking a random number, $0 < r < 1$, and for a branch point to exist requiring that $r < r_1$ (non-scission) or $r < r_4$ (scission).

The length of the (first) primary polymer, n, is determined in relation to the previously sampled number of scission points, i, by sampling from the distribution $p^{wt}(n|i)$ also shown in Table 1. Finally, the number of backbone branch points follows from n and the branching density ρ_b using Eqs. (29) and (30).

3.4.7. Backbone branch point loop

Any primary polymer may turn out to possess branch points on its backbone, as identified in the above procedure, Eqs. (29) and (30). To such branch points primary polymers are attached by one of their end points. Hence, the characteristics of such primary polymers belong to the class of those that possess at least one branch point. In the backbone branch point loop the length, the number of backbone branch points and the connectivity of the

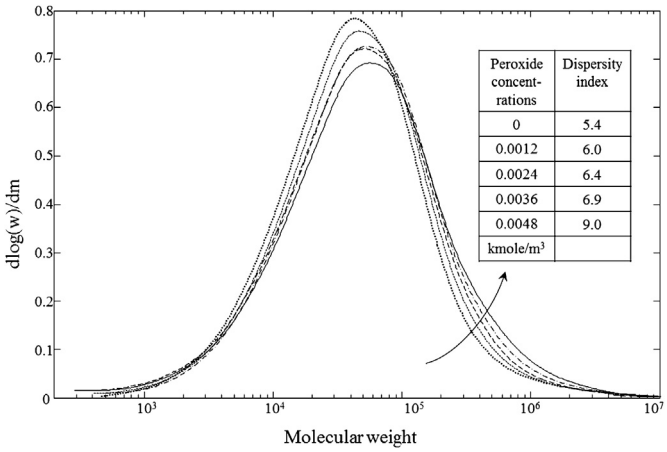

Fig. 9. Molecular Weight Distributions of 5 HD Polyethylene (PE 539123) samples from SEC-MALS, one unmodified, four modified with different peroxide concentrations. The leftmost distribution (dotted line) represents the untreated PE. The MWD's of the 4 samples chemically modified in the ZSK200 twin-screw extruder show a broadening and a higher dispersity index with increasing peroxide concentration.

second end point have to be determined. The branch point of the attached end necessarily has to be created from a previous vinyl end. Again, it is important to know whether it originates from scission and subsequent reaction to a vinyl end, or it represents an initially present vinyl end, not resulting from scission. The identity of the attached end of the primary polymer, scission or no scission, determines the other end's connectivity and its length [27,28].

The following question now arises. Given the fact that the attached end of the primary polymer is a branch point, what is the probability that it is a scission or non-scission point? Since all branch points come from vinyl ends, the answer must be that this probability is equal to the ratio between the amounts of the two different types of vinyl ends reacting to branch points. The total amount of terminal vinyl groups originating from *scission* reacting to branch points is calculated as follows, see also Fig. 8. The total amount of scission ends produced, either terminal vinyl or as primary radicals, is equal to $2k_s \int_0^\tau \lambda_1^s \mathrm{d}t$. Since the fraction of all scission ends reacting to branch points has been derived above as r_4 according to Eq. (28), the total amount of branch points originating from scission is equal to $2r_4k_s \int_0^\tau \lambda_1^s \mathrm{d}t$. Now, the amount of initially present terminal vinyl groups in virgin PE reacting to branch points has from Eqs. (23) and (24) been calculated to equal $k_{vs} \int_0^\tau \mu_1^{v0} \lambda_1^s \mathrm{d}t$. Thus, the probability that a branch points originates from scission becomes:

$$r_5 = \frac{2r_4k_s \int_0^\tau \lambda_1^s \mathrm{d}t}{2r_4k_s \int_0^\tau \lambda_1^s \mathrm{d}t + k_{vs} \int_0^\tau \mu_1^{v0} \lambda_1^s \mathrm{d}t} \tag{31}$$

Once the identity of the attached end of the primary polymer, scission or no scission, is known the other end's identity and its length may be determined. These properties are obtained by sampling from *conditional* distributions that have been derived from the semi-analytical approach before [27,28], see Table 1. The number weighted (superscript *nr*) probability $p^{nr}(i|j)$ represents the chance, for a primary polymer under the condition that its sampling end equals j (= 0 for non-scission, 1 for scission), that the other chain end's identity equals i. If the scission/non-scission identity of the other end points is known, scission or non-scission, the probability that they are branch points again follows using the probabilities r_1 and r_4 obtained above, by Eqs. (25) and (28), resp. A branch point is present, if a random number r ($0 < r < 1$) [$<r_1$ (non-scission) or $< r_4$ (scission). The length, n, follows by sampling from the conditional length distribution $p^{nr}(n|i,j)$ (i, j are 0 or 1), see Table 1. Finally, as in the other loop, the number of backbone branch points follows from n and the branching density ρ_b using Eqs. (29) and (30).

4. Results and discussion

4.1. SEC-MALS data

The measured SEC-MALS curves for a High-Density PE-grade from Sabic, PE 539123, subjected to varying peroxide-concentrations in the ZSK200 twin-screw extruder between 0.0012 and 0.0048 kmol/m^3, are shown in Fig. 9.

4.2. Starting conditions simulations

Simulations have been performed using the measured Molecular Weight Distribution of the untreated Polyethylene sample as the input distribution (Fig. 9). We have assumed ideal mixing, so the system is acting as an ideally mixed batch reactor. In practice, non-ideal mixing might be at hand, as was the case in the (strong) degradation of Polypropylene in our previous study [3]. However, in the present case of mild modification of PE ideal mixing seems to be a good assumption.

Table 2
Kinetic data and concentrations for ZSK200 twin-screw extruder conditions.

Rate coefficient/species concentration	Symbol	Value	Units
Initial initiator concentration	$I_2(0)$	0.0012–0.0048	kmol.m^{-3}
PE density	ρ	750	kg.m^{-3}
Number average MW virgin PE (average chain length)	M_n ($\overline{n}_n$)	16.7 (596)	kg.mol^{-1}
PE concentration ($\mu_1/\overline{n}_n$)	μ_0	1.6×10^{-3}	kmol.m^{-3}
PE concentration (ρ/M, $M = 28$)	μ_1	26.8	kmol.m^{-3}
Initial fraction vinyl chain ends	$r_=(0)$	0.1	
Conversion of vinyl ends	$\eta_=$	0.23–0.79	
Average res. time ZSK200 twin-screw extruder	τ	30	s
Initiator dissociation (Perkadox 14, 210 °C)	k_d	1	s^{-1}
Hydrogen abstraction by initiator radical	k_{ht}	10	m^3.kmol^{-1} s^{-1}
Hydrogen abstraction by primary radical	k_{htp}	0	m^3.kmol^{-1} s^{-1}
Disproportionation coefficients (primary, secondary, tertiary radicals)	k_{td}, k_{tds}, k_{td},	10^{13}	m^3.kmol^{-1} s^{-1}
Vinyl to secondary radical coupling	k_{vs}	3.5×10^8	m^3.kmol^{-1} s^{-1}
Random scission	k_s	$0–7.5 \times 10^4$	s^{-1}

Some of the input data have been inserted as fixed values, like the density of the modification conditions, $\rho = 750$ kg/m^3, from which the first moment as defined by Eq. (9) is calculated as $\mu_1 = \rho/M = 26.8$ kmol/m^3 ($M = 28$, molecular weight of Ethylene). It has been assumed that 10% of the linear chain ends carries a terminal double bond. This value is based on the FTIR measurements. The starting concentration of initiator, $I_2(0)$, was varied around those applied in the PE modification experiments. Reaction time, τ, was not varied, but constantly taken as 30 s, according to the experiments. The initiator dissociation rate was assumed to invariably equal that of Perkadox at 210 °C. Neither the coefficient of hydrogen abstraction was varied, whose value was taken from our previous PP degradation study to be constantly 10 kg/(kmol.m^3). Hydrogen abstraction by primary radicals has been attributed a negligible role, since not many primary radicals are present. The only source of these radicals is random scission, which will turn out to be at a low level, as is shown below. The kinetic coefficients for vinyl to secondary radical coupling, k_{vs}, and for scission were used as adjustable parameters to attain the best fit with experimental data. All these data have been summarized in Table 2.

4.3. Simulation results

MC simulations generate populations of around 600,000 molecules. The numbers of monomer units and primary polymers (equal to number of branch points plus 1) of each molecule are registered. The MWD is constructed as a histogram with (logarithmic) molecular weight bins. Concerning the shape of the MWD's the simulations have revealed the following. The MWD appears to be most susceptible for the vinyl to secondary radical coupling coefficient, k_{vs}, while the role of scission turned out to be minor, although not negligible. Varying the scission coefficient appears to be important to find a better fit in the *tail* of the MWD. As regards the coupling coefficient, k_{vs}, the best MWD fit was found, for the 4 different initiator concentrations, for a value of 3.5×10^8 m^3.kmol^{-1} s^{-1}. Note that according to the branching mechanism vinyl ends are consumed and changed into branch points. According to the kinetic model during the modification process between 23% ($I_2(0) = 0.0012$ kmol m^{-3}) and 79% ($I_2(0) = 0.0048$ kmol m^{-3}) of these vinyl ends is consumed, which is in agreement with the FTIR measurements. Fig. 10 shows the 4 MWD's from simulations and SEC-MALS. The MWD of virgin PE is shown for reference. The molecular weight averages have been summarized in Table 3. One may observe that through chemical modification the MWD of PE becomes broader; the long tail does not undergo a major change. For all of the concentrations an almost perfect fit is found between measured and simulated MWD. This confirms the importance of the vinyl to secondary coupling mechanism in PE modification, as was experimentally found in an entirely different way, in the EPR-study by Camara et al. [1].

The role of scission is shown in Fig. 11, where we plotted the tail of the MWD's for initiator concentrations $I_2(0) = 0.0024$ and 0.0048 kmol kg^{-1}. From the SEC-MALS curves one may conclude, as far as the accuracy of the data permits, that the tail of the MWD hardly is changed during the modification process. If in the simulations scission is assumed to be absent, as in the study by Brandolin et al. [5] the tail of the MWD is clearly extended to much higher weights, around 2×10^7. Since, we do not see this in the SEC-MALS, it must be concluded that scission is acting here and preventing tail extension. This is confirmed by considering the average MW values in Table 3. The values obtained with MC assuming scission are generally closer to the measured MW, than those assuming scission to be absent. We found, from the 4 measured MWD's, that a value of the scission coefficient, k_s, equal to 7.5×10^4 s^{-1} leads to the best fit for the MWD tail. This corresponds to an average *scission probability*, ρ_s, for the highest initiator concentration of 1.3×10^{-5} (scission events per monomer unit). This is a factor 20 lower than the average *branching density* (see below), ρ_b.

Finally, the branching density as a function of molecular weight is calculated from the Monte Carlo simulations. This density

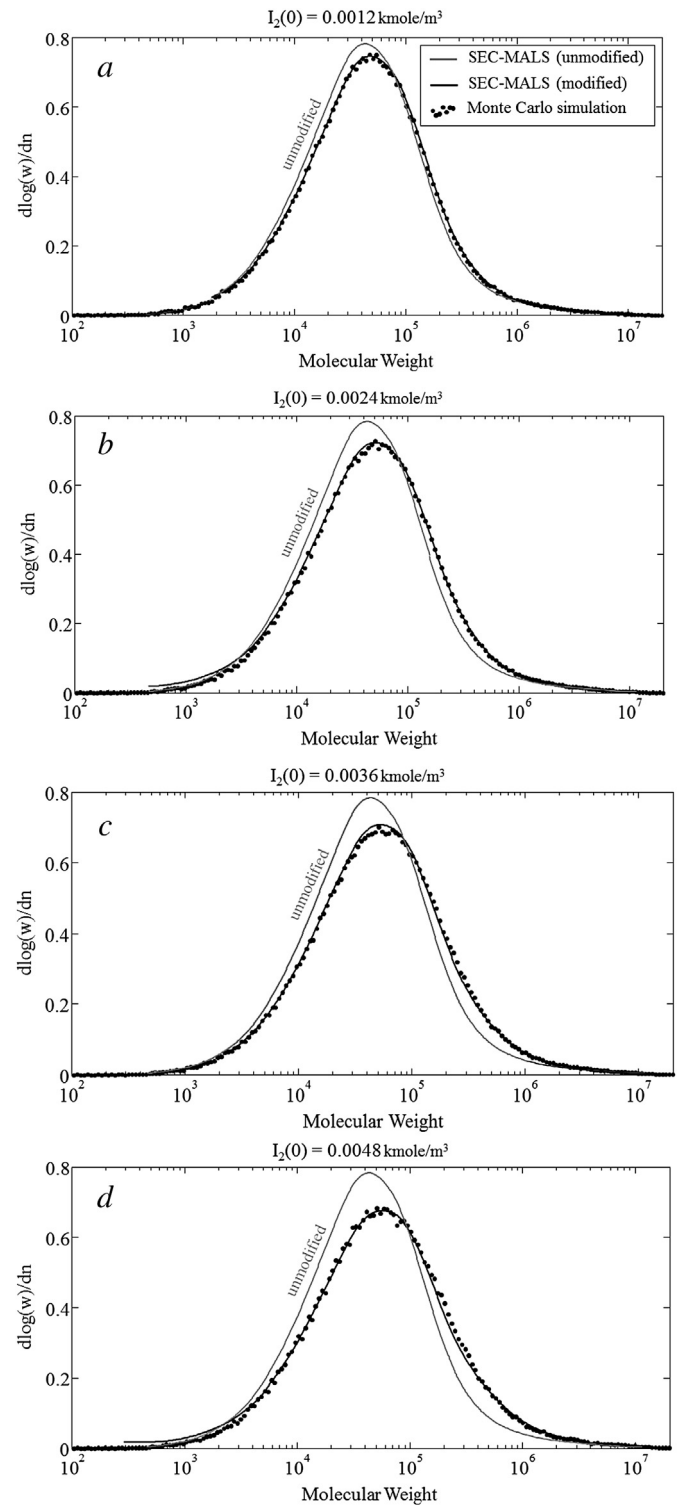

Fig. 10. a–d. MWD's for samples 1–4 with varying initiator concentration, $I_2(0)$. MWD of unmodified PE is shown (in gray) for reference. The MC simulations assuming vinyl to secondary radical coupling with $k_{vs} = 3.5 \times 10^8$ m^3.kmol^{-1} s^{-1} and random scission with $k_s = 7.5 \times 10^4$ s^{-1} show excellent agreement with the SEC-MALS measurements of modified PE (black drawn curves).

Table 3
Number (M_n) and weight (M_w) average molecular weights and dispersity index (Đ) for virgin (sample 0) and modified (samples 1–4) PE according to the SEC-MALS measurements and the MC simulations (with/without scission). These are the averages of the MWD's shown in Fig. 10.

	Samples													Units
	0	1			2			3			4			
	SEC-MALS	SEC-MALS	MC scis.	MC non- scis.	SEC-MALS	MC scis.	MC non- scis.	SEC-MALS	MC scis.	MC non- scis.	SEC-MALS	MC scis.	MC non- scis.	
M_n	**16.7**	**14.5**	17	17	**16.4**	17.4	17.4	**16.4**	18.1	18.2	**11.2**	18.5	18.6	kg.mol^{-1}
M_w	**116**	**123**	124	129	**136**	122	142	**136**	141	159	**150**	150	180	kg.mol^{-1}
Đ	**7.0**	**8.5**	7.3	7.5	**8.3**	7.0	8.0	**8.3**	7.8	8.7	**13.4**	8.1	9.7	

Experimental values are in bold.

distribution is derived from the 3-dimensional concentration distribution $P(n,v,b)$ as formulated in Eq. (21):

$$\rho_b(n) = \frac{1}{n}\sum_{v=0}^{\infty}\sum_{b=0}^{\infty} bP(n,v,b) \tag{32}$$

This $\rho_b(n)$ is derived from the populations of generated molecules by collecting both the numbers of branch points (one less than the number of primary polymers) and the numbers of monomer units of all molecules in a molecular weight interval. Summing up both numbers and taking the quotient provides the branching density for that interval. The resulting branching density distribution is shown for two initiator concentrations in Fig. 12. Note that the *averages* for the branching density, ρ_b, according to Eq. (29), amount to 1.6×10^{-4} (sample 2) and 2.8×10^{-4} (sample 4). One observes a maximum of the branching density at around an MW of 300 kg.mol^{-1}. Due to this shape the longest chains, having a lower branching density, possess around 180 branch points (sample 4). The lower branching density at longer chain lengths also implies that the increase of chain length by branching for those chains is somewhat less significant.

Finally, in Fig. 13 we show the branched architecture of one example molecule from the population (typically 600,000 molecules) for the conditions of sample 4. This molecule counts 82,551 monomer units, 30 branch points. The lengths of the 31 primary polymers are shown. The generation at which the primary polymers are becoming attached is indicated with lines of decreasing thickness; in this example it took 7 generations to produce the molecule. It contains two very long molecules, one introduced in generation 0 (length 46,792) and one in generation 5 (12,471). The attachment of one small segment (37) in generation 7 concludes the process. The first primary polymer possesses a non-connected scission point. The generation 1 primary polymers of lengths x and y are connected by a (former) scission point. Note, that with a scission probability, ρ_s, of around 10^{-5} one would expect on average just one scission point for this molecule, as compared to the total of three in this case. In this molecule all the vinyl ends have been converted into branch points. No unreacted vinyl ends are present anymore, although this would have been possible.

The attachment of one small segment (37) in generation 7 concludes the process. The first primary polymer possesses a non-connected scission point. The generation 1 primary polymers of lengths 112 and 148 are connected by a (former) scission point. Note, that with a scission probability, ρ_s, of around 10^{-5} one would expect on average just one scission point for this molecule, as compared to the total of three in this case. In this molecule all the vinyl ends have been converted into branch points. No unreacted

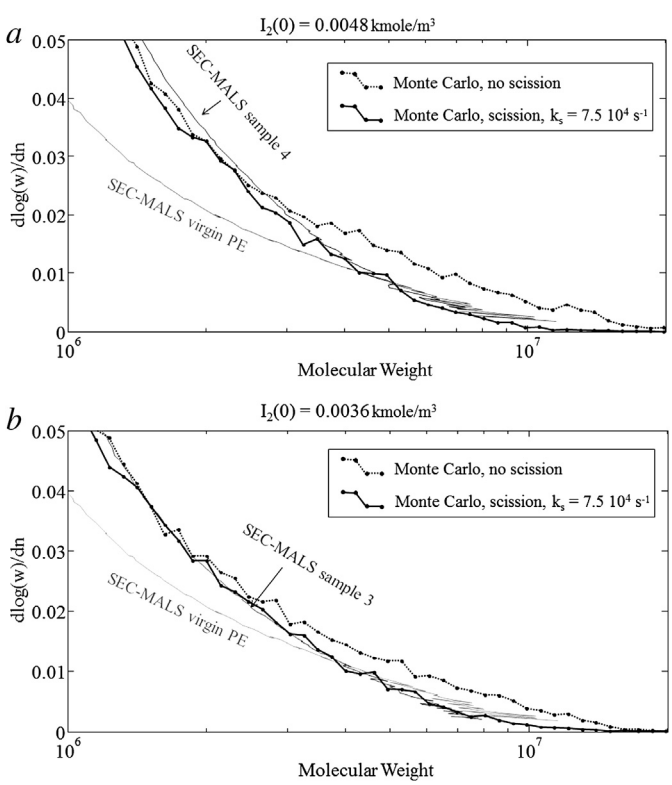

Fig. 11. a,b. Effect of scission on the tail of the MWD, for two initiator concentrations. The measured MWD (SEC-MALS) does not show a significantly extended tail. If no scission is assumed in the MC simulations, the tail is clearly extended. Assuming mild scission, with $k_s = 7.5 \times 10^4$, a fair agreement between the tails of the measured and calculated MWD is obtained; $k_{vs} = 3.5 \times 10^8$ m^3.kmol^{-1} s^{-1}.

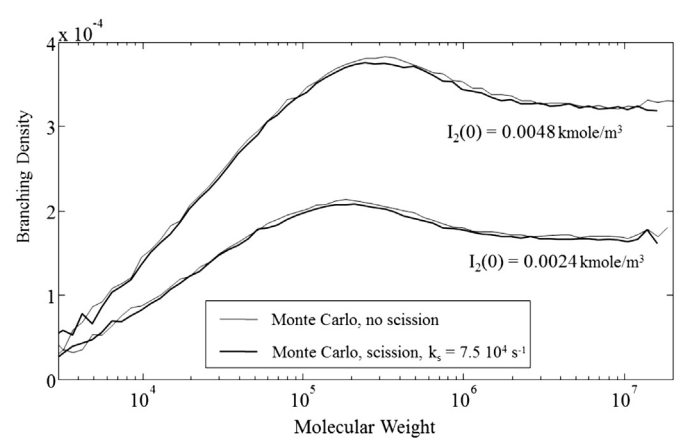

Fig. 12. Branching density as a function of MW from Monte Carlo simulations for conditions of sample 2 and 4. The effect of scission is small. Average branching density ρ_b equals 1.6×10^{-4} (sample 2) and 2.8×10^{-4} (sample 4). The maximum number of branch points per molecules for the longest chains is around 180. $k_{vs} = 3.5 \times 10^8$ m^3.kmol^{-1} s^{-1}.

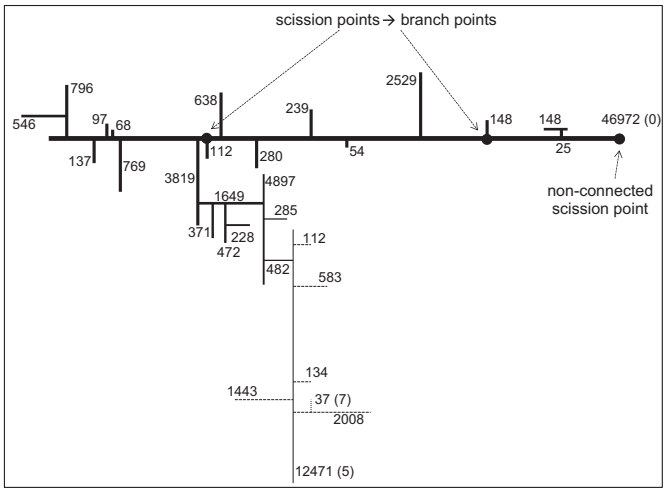

Fig. 13. Example molecule for sample 4, monomer units: $n = 82{,}551$, branch points: $b = 30$. Primary polymers of subsequent generations in decreasing thickness. Two long chains: generation 0: 46,972, generation 5: 12,471; last generation (7): small branch (37). Two H-shape branching structures visible. Three scission points, two connected, one non-connected. No unreacted vinyl ends.

vinyl ends are present anymore, although this would have been possible.

The example of the branched architecture of a molecule created by chemical modification of PE shows that the MC model gives access to properties of importance for characterization and rheology that are based on the branching topology. In Iedema et al. [27] for different branched polymer topologies we have shown how to infer the contraction factor of the *radius of gyration* as well as *rheological* qualifiers (seniority, priority) from populations of topologies using graph theory. The same procedure has been followed in a recent Science paper [2], where it was shown how the generated populations of branching topologies are employed for predicting the complex rheological behavior of the polymer melt.

Although in the present PE modification study the branching distribution in itself was not directly experimentally verified, the underlying kinetic mechanism leading to the specific branching topology has indeed been validated through our MC model. Hence, we conclude that the above mentioned topology-based properties, accessible through available computational methods, possess a clear kinetic basis. Moreover, since these properties in themselves are amenable to experimental verification, as was shown by Liu et al. [16], such calculations would form an interesting extra link to experimental data.

5. Conclusions

PE modification experiments have been carried out within a ZSK200 twin-screw extruder with Perkadox 14 as the peroxide used. The MWD of the virgin PE and the treated samples were obtained with SEC-MALS. With FTIR and NMR the presence of vinyl end groups was identified, amounting to about 10% of all chain ends. A Monte Carlo simulation model computing MWD has been constructed allowing for all of the usual modification reactions: initiator dissociation, hydrogen abstraction, termination by disproportionation. The existence of *random scission* has also been accounted for. This gives rise to 'primary polymers', the usual [17] linear building blocks of the MC simulation, that have undergone scission and therefore have lengths depending on the number of scission ends. Several *branching* mechanisms have been proposed for PE modification before [5–15], but here we assume that the most important branching reaction is the coupling of a vinyl end to a secondary radical site. This yields a tertiary radical branch point that is converted in a non-radical site by disproportionation.

The rate coefficients for vinyl to secondary radical coupling and for random scission, k_{vs} and k_s resp., have been employed as adjustable parameters to fit the calculated MWD's to those measured by SEC-MALS. Perfect agreement was found for the complete experimental series with different peroxide concentrations using the values $k_{vs} = 3.5 \times 10^8$ $m^3 kmol^{-1}$ s^{-1} and $k_s = 7.5 \times 10^4$ s^{-1}. The latter value corresponds to relatively mild scission, which was seen to explain the apparently unchanged shape of the MWD tail in the SEC-MALS results. The fact that we could reproduce the MWD's with just one branching mechanism, being the vinyl to secondary radical site coupling, is well in line with an earlier study of PE modification by EPR [1]. In another study of PE modification [5] random scission has been completely ignored. Although we did not find this mechanism to dramatically affect the main part of the MWD, our findings do not justify ignoring scission.

The MC model allows computing the average numbers of branch points and branching density as a function of the molecular weight. Interestingly, a maximum in the branching density was found at around an MW of 300 $kg.mol^{-1}$. Due to this effect the maximum number of branch points found in the longest molecule is around 180 (highest initiator concentration). The average probability of a monomer unit to become a branch point turns out to be a factor 20 higher ($\rho_b = 2.8 \times 10^{-4}$) than the probability to undergo a scission reaction (ρ_s). The branching distribution could not yet be compared to experimental data from SEC-MALS or NMR. However, our model allows computing branching topologies, as was shown by an example molecule, which form the computational basis for inferring properties like radius of gyration contraction factors and rheological qualifiers. Hence, the explicit branching topologies form an extra link to experimentally accessible properties. In forthcoming publications we will more thoroughly investigate the branching distribution using direct or indirect experimental information concerning branching (topologies). This would include studies of PE modification, where a certain amount of *initial* branching is present. The MC model is easily extendable to incorporate such a condition.

Acknowledgments

The authors want to sincerely thank Dr. Jacques Tacx of Sabic Europe, Geleen, NL, for generously offering his assistance in all discussions concerning the application of SEC-MALS to branched polymers.

References

[1] Camara S, Gilbert BC, Meier RJ, van Duin M, Whitwood AC. Polymer 2006;47:4683–93.
[2] Read DJ, Auhl D, Das C, den Doelder J, Kapnistos M, Vittorias I, et al. Science 2012;333:1871–4.
[3] Iedema PD, Remerie K, van der Ham M, Biemond E, Tacx J. Chem Eng Sci 2011;66(22):5474–86.
[4] El Mabrouk K, Scott Parent J, Chaudhary BI, Cong R. Polymer 2009;50:5390–7.
[5] Brandolin A, Sarmoria C, Failla MD, Valle EM. Ind Eng Chem Res 2007;46:7561–70.
[6] Cheung PC, Balke ST. Ind Eng Chem Res 1997;36:1191–201.
[7] Gloor PE, Tang Y, Kostanska AE, Hamielec AE. Polymer 1994;35(5):1012–39.
[8] Sezgi NA, Cha WS, Smith JM, McCoy BJ. Ind Eng Chem Res 1998;37:2582–91.
[9] Pinheiroa LA, Chinelatto MA, Canevarolo SV. Polym Degrad Stabil 2004;86:445–53.
[10] Hinsken H, Moss S, Pauquet J-R, Zweifel H. Polym Degrad Stabil 1991;34:279–93.
[11] Shroff RN, Mavridis H. Macromolecules 1999;32:8454–64.

[12] Garcia-Franco CA, Lohse DJ, Robertson CG, Georjon O. Eur Polym J 2008;44:376–91.
[13] Helmstedt M, Stejskal J, Burchard W. Macromol Symp 2000;162:63–79.
[14] Vega JF, Martinez-Salazar J. Polym Bull 2003;50:197–204.
[15] Scaffaro R, La Mantia FP, Botta L, Morreale M, Dintcheva NTz, Mariani P. Pol Eng Sci 2009;49:1316–25.
[16] Liu J, Yu W, Zhou W, Zhou C. Polymer 2009;50:547–52.
[17] Tobita H. J Pol Sci Part B Pol Phys 2003;31:1363–71.
[18] Tobita H. Macromol Theory Simul 1996;5:1167–94.
[19] Tobita H. J Pol Sci Part B Pol Phys 2001;39:391–403.
[20] Tobita H. Polymer 1995;36:2585.
[21] Tobita H, Hatanaka K. J Pol Sci Part B Pol Phys 1995;33:841–53.
[22] Tobita H. Polymer 1997;38:1705–17.
[23] Tobita H. J Pol Sci Part B Pol Phys 1994;32:901–10.
[24] Tobita H. J Pol Sci Part B Pol Phys 1994;32:911–9.
[25] Tobita H, Hatanaka K. J Pol Sci Part B Pol Phys 1996;34:671–8.
[26] Tobita H. Macromolecules 1996;29:3000–9.
[27] Iedema PD. Polymer 2011;52:3537–49.
[28] Iedema PD. Macromol Theory Simul 2012;21:166–86.
[29] Kryven I, Iedema PD. Macromol Theory Simul 2012;22:89–106.
[30] Tackx P, Tacx JCJF. Polymer 1998;39:3109–13.
[31] De Groot AW, Hamre WJ. International GPC symposium proceedings. Milford, M.A: Waters Chromatography Division, Millipore Corp.; 1991. p. 353.
[32] Iedema PD, Hoefsloot HCJ. Macromolecules 2004;37:10155–64.